DMTA Based Investigation of Hygrothermal Ageing of an Epoxy System Used in Rehabilitation

Guijun Xian,[1,2] Vistasp M. Karbhari[1,2]

[1]*Department of Structural Engineering, University of California San Diego, La Jolla, California 92093-0085*
[2]*Materials Science & Engineering Program, University of California San Diego, La Jolla, California 92093-0085*

Received 15 June 2006; accepted 10 September 2006
DOI 10.1002/app.25576
Published online in Wiley InterScience (www.interscience.wiley.com).

ABSTRACT: Dynamic mechanical thermal analysis (DMTA) techniques were used to investigate the moisture uptake and ageing of an ambient temperature cured epoxy used in the external strengthening of deteriorating concrete structures. Since the process is conducted under field conditions, cure does not progress completely prior to exposure to environmental conditions. Resin samples are immersed in deionized water at 23, 40, and 60°C, as well as in 5% NaCl and concrete based alkali solution at 23°C for periods up to 24 months. Diffusion coefficients increase with increase in temperature of immersion, but the maximum/equilibrium moisture content over the period of time is seen to be largely independent of temperature of immersion and type of solution. Glass transition temperature was found to decrease with increasing moisture uptake, with competing effects of cure progression and plasticization in the early periods of exposure, followed by hydrolysis and irreversible deterioration over longer periods of time. Splitting of the T_g of samples aged in deionized water and alkali solution indicate the formation of biphasic structures and drying of the network structure during DMTA. A biphasic structure indicating differently plasticized phases in the skin regions, which is different from the response in the bulk, is seen in samples immersed in salt solution. © 2007 Wiley Periodicals, Inc. J Appl Polym Sci 104: 1084–1094, 2007

Key words: glass transition temperature; degradation; hygrothermal ageing

INTRODUCTION

Fiber reinforced polymer (FRP) composites are increasingly being used in marine and civil infrastructure applications, where the constraints of cost, anticipated service-life, and inspection and maintenance schedules are very different from those seen in aerospace applications. Because of considerations related to the type of structures and the cost, the processes used for fabrication are often very different from the highly controlled prepreg based autoclave cure process used conventionally in the aerospace arena. In a number of applications such as in the rehabilitation of civil infrastructure through the external bonding of FRP composites, processing is done in an uncontrolled outdoor environment with concrete serving as the substrate. In such applications, the resin system and the ensuing composite is subject to a range of environments including exposure to humidity, temperature variations, water, and other aqueous solutions over extended periods of time. Most polymers are known to absorb water and the potential deterioration in strength resulting from this is well documented. Since rehabilitation is primarily conducted under ambient conditions, there is also potential for under-cure or a slow progression of cure, both of which increase the potential for moisture induced degradation. Since the application is usually conducted to strengthen or increase the life of primary structural components that are expected to have long postrehabilitation service-lives, it is crucial that a better understanding is developed vis-à-vis the long-term effects of moisture uptake on durability and service-life performance of this class of polymers and composites.

Although some researchers have suggested that the level of water absorption is determined by the available free volume of the polymer,[1–4] others have emphasized the crucial role of hydrophilic groups for both water absorption and diffusion.[5–9] Different models have been used to describe the diffusion process ranging from the simplest case, where diffusion is driven by the water concentration gradient described by a Fickian model,[10] to the more complex stress-dependent,[11] history dependent,[12] and dual phase,[11,13] diffusion models. While Fickian diffusion is often assumed, diffusion in thermosetting polymers often involves both the concentration-gradient driven Fickian diffusion, and a time-dependent relaxation process, resulting in phased- or pseudo-Fickian response.

Water molecules are believed to exist in epoxies either in voids and microcenters, as ''free'' water molecules or dispersed in the bulk, as ''bound'' water molecules.[1,14–16] ''Free'' water is not expected to influence molecular mobility and thus does not, in the

Correspondence to: V. M. Karbhari (vkarbhari@ucsd.edu).

Journal of Applied Polymer Science, Vol. 104, 1084–1094 (2007)
© 2007 Wiley Periodicals, Inc.

short-term, cause any plasticization.[17] However, the ''bound'' water disrupts the interchain hydrogen bonds in an epoxy network, promoting mobility of molecular segments, and thus contributing to more-or-less reversible plasticization.[14,18] Zhou and Lucas[18] reported that tightly bound water molecules contribute to an increase in the glass transition temperature through the formation of a secondary crosslink network. Apart from the mechanisms of largely reversible plasticization and apparent cure progression, absorbed water can also cause irreversible damage such as chain scission, hydrolysis, crack initiation, crack growth, and subsequent loss of material.

The combination of incomplete cure, harsh and changing exposure conditions resulting from outdoor exposure, need for very long service-lives (25+ years even for rehabilitation), poor inspection and maintenance (when compared with that of the aerospace and marine areas), and the overall emphasis on cost makes the robust use of FRP materials in civil infrastructure applications a significant challenge. There is a significant need to develop a better and more comprehensive understanding of environmental effects on the specific classes of materials used in these applications, especially as these are related to moisture induced deterioration. This article discusses moisture uptake and subsequent effects on an epoxy system commonly used in the field rehabilitation of concrete structures through the external bonding of composites.

EXPERIMENTAL

An ambient temperature cure two-part epoxy system formed of a 4,4′-isopropylidenephenol-epichlorohydrin used with an aliphatic amine hardener in a 2 : 1 ratio was considered in the study. The system is representative of resin systems commonly used for field rehabilitation with a gel time of about 60 min at 23°C and a viscosity of 800 cps. Neat resin panels of 5-mm thickness were cast and allowed to cure without application of pressure. The density of the cured resin was 1.22 g/cc. Prior to initiation of tests and exposure, samples were conditioned for 30 days at 40°C and 30% relative humidity (RH) at the end of which the weight change, measured periodically through that time, was less than 0.05%.

Specimens were immersed in deionized water at 23, 40, and 60°C and in 5% NaCl solution at 23°C (representing a salt water or saline environment), in concrete based alkaline solution[19] at 23°C, and were also stored under controlled conditions of 23°C and 30% RH.

Absorption

Specimens of size 25.4 × 25.4 × 5 mm^3 were used for absorption using gravimetric means. At periodic intervals, specimens were removed from the exposure environments, dried superficially using paper tissue, weighed, and then returned to solution. For each set a minimum of 10 specimens were used.

Desorption

Selected specimens aged in the exposure conditions for a period of two years were carefully cut using a microtome to thicknesses of 0.5 mm and the central regions were used for desorption characterization. Specimens were surface dried, weighed, and then reconditioned in an oven at 40, 60, and 80°C until a stable condition of weight was achieved. A minimum of three specimens were used for each time period and condition at each of the three temperatures used for desorption.

Dynamic mechanical thermal analysis

Specimens of 35 × 9 × 5 mm^3 were tested in a dynamic mechanical thermal analysis (DMTA) after removal from exposure conditions at periodic intervals at a frequency of 1 Hz and a strain of 0.025% at a heating rate of 5°C/min between 25 and 160°C in three-point flexure mode. For each condition, three specimens were used. Tests on desorbed specimens (25 × 5 × 0.5 mm^3) were conducted in a tension mode at a frequency of 1 Hz and a strain of 0.025% at a heating rate of 5°C/min between 25 and 160°C. For purposes of analysis, the peak of the loss tangent curve was used as an indicator of the glass transition temperature.

Differential scanning calorimetry

Samples (10–20 mg) cut from the films were used for differential scanning calorimetry (DSC) tests. Samples were heated at a rate of 10°C/min between −20 and 160°C. Subsequent to the first run, specimens were cooled back to −20°C at a rate of 2°C/min and then heated again under the same conditions as the initial run. Nitrogen at the level of 10 mL/min was used.

RESULTS AND DISCUSSION

As shown in Figure 1, moisture uptake in samples aged under ambient conditions (23°C and 30% RH) does not achieve saturation after even two years of exposure, with a trend that clearly deviates from Fickian response. It is noted that Deneve and Shanahan reported similar moisture uptake behavior, which they termed as sigmoidal, for a filled epoxy system aged at ~ 100% RH.[20] This response can be related to incomplete cure and relaxation of the glassy state of the resin.

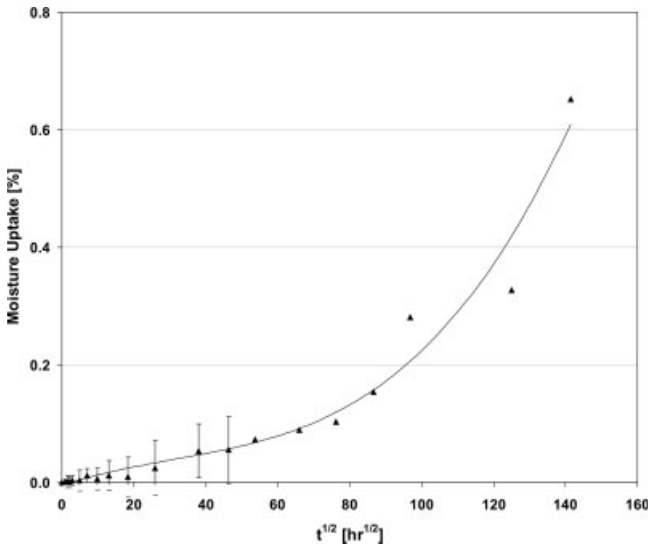

Figure 1 Moisture uptake under ''control'' conditions (23°C and 30% RH).

Moisture uptake curves as a result of immersion in deionized water (at 23, 40, and 60°C) and salt and alkali solutions (both at 23°C) are depicted in Figure 2. The response as a result of immersion in deionized water at 40 and 60°C is clearly Fickian in nature, with similar saturation levels within bounds of statistical deviation ($\sim$ 3.99%). The uptake curves for the three solutions at 23°C are almost identical. Within the 24-month period of immersion, the uptake in the other three conditions (deionized water, salt and alkali solution, all at 23°C) does not reach full equilibrium water uptake, but is seen to approach the levels shown at the two higher temperatures, which could be assumed to be the level of saturation content based on the epoxy system possessing a moderately polar network.[21]

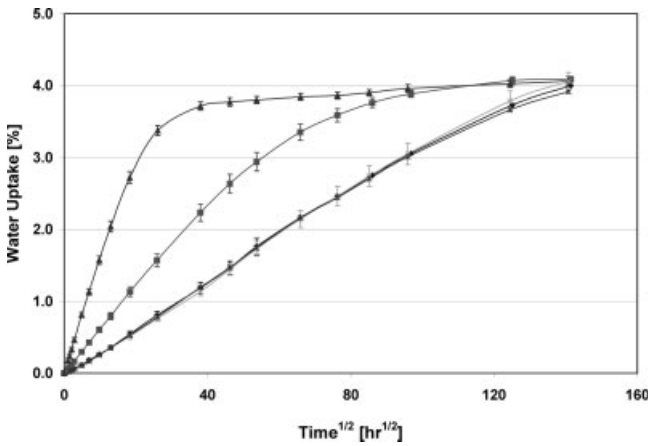

Figure 2 Moisture uptake curves (◆; deionized water at 23°C; ■, deionized water at 40°C, ▲; deionized water at 60°C; X, alkali solution at 23°C; O, salt solution at 23°C).

Following the classical approach to Fick's second law, the apparent diffusivity (D_a) is calculated using

$$D_a = \frac{\pi}{16}\left(\frac{h}{M_\infty}\right)^2\left(\frac{dM}{dt^{1/2}}\right)^2 \quad (1)$$

where h is the thickness of the specimen, t is the exposure time, and M_∞ is the saturation water uptake level. Values of D_a corresponding to the various immersion conditions are presented in Table I. Because of the dimensions of specimens used, the application of an edge correction is necessary[22] and the actual sample diffusivity can then be determined as

$$D_x = D_a\left(1+\frac{h}{l}+\frac{h}{w}\right)^{-2} \quad (2)$$

where l and w are the sample length and width, respectively. The corresponding values of D_x are also given in Table I. The change in diffusivity with temperature of immersion is consistent with results reported earlier,[23,24] including that based on a study of carbon fiber reinforced composites using the same resin for purposes of infrastructure rehabilitation.[24] Note that the activation energy, E, for diffusion can be calculated according to the Arrhenius relationship

$$D_x = D_o\ \exp(-E/RT) \quad (3)$$

where D_o is a constant, R is the universal gas constant, and T is the absolute temperature in Kelvin, an activation energy of 16.7 kcal/mol (69.9 kJ/mol) can be calculated for the material used in this investigation, which is in close agreement with the value of 16.4 kcal/mol (68.49 kJ/mol) reported by Abanilla et al.[24] for immersion in deionized water, and the value of 19.1 kcal/mol (14.4 80 kJ/mol) reported by Deneve and Shanahan[20] for an epoxy system at $\sim$ 100% RH. It is noted that there is only a very small difference in overall uptake response accruing from immersion in the three different solutions at 23°C, suggesting that the presence of NaCl and alkali salts do not have a perceptible effect on moisture uptake in this epoxy system.

Desorption response

A typical plot for desorption, showing the initial rapid decrease in weight due to loss of moisture, fol-

TABLE I
Diffusion Coefficients of the Epoxy Resin under Different Immersion Conditions

Immersion condition	D_a (10^{-6} mm^2/s)	D_x (10^{-6} mm^2/s)
23°C, Deionized water	0.083	0.044
40°C, Deionized water	0.29	0.152
60°C, Deionized water	1.916	1.01
23°C, Alkali solution	0.081	0.043
23°C, Salt solution	0.082	0.043

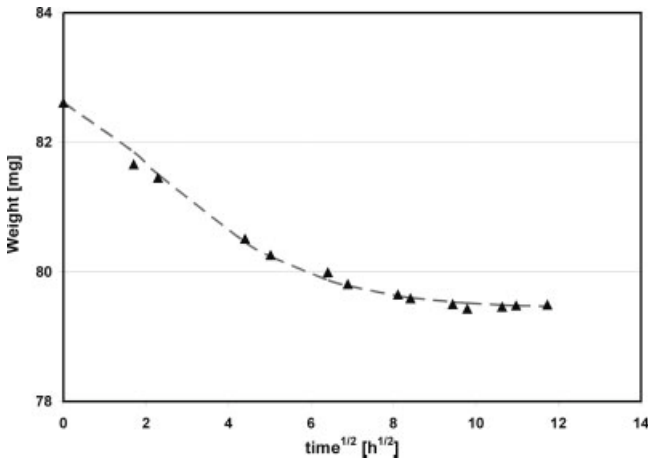

Figure 3 Typical curve resulting from drying specimens immersed in salt solution (▲, measured data; ----, eq. (4)).

lowed by an asymptotic trend towards an equilibrium level is shown in Figure 3, indicating a reverse Fickian response. To obtain the equilibrium water content in loss after desorption and the diffusivity of water, in the present work, the diffusion equation used in[22] can be reformulated, so that D and M_∞ can be obtained as

$$m = m_0 - m_0\left(1 - \frac{1}{1 + M_\infty}\right) \left\{1 - \exp\left[-7.3\left(\frac{Dt}{h^2}\right)^{0.75}\right]\right\} \quad (4)$$

where m is the film weight at drying time t, m_0 is the original weight of the wet film (corresponding to a drying time of 0), and M_∞ is the equilibrium desorbed moisture content. The dashed line in Figure 3 shows the fit achieved using eq. (4).

Since thinner sections are cut from the 5-mm thick specimens, it is important to verify that thickness has no effect on the final desorption parameters. Figure 4 shows the effect of specimen thickness on diffusivity and M_∞ related to desorption for samples aged in deionized water at 40°C for 24 months. It can be seen that the equilibrium water content is independent of the thickness, suggesting that the water has penetrated uniformly through the specimens over the period of investigation. Although the values of apparent diffusivity (D_a) increase with the thickness, the actual diffusivity determined after application of edge correction (D_x) is largely independent of the thickness.

Desorption parameters, D and $M_{\infty,}$ for aged epoxy samples dried at 40, 60, and 80°C are listed in Table II. At the same drying temperature, all specimens show very similar values of D_x and M_∞, indicating that these characteristics are not affected by the previous ageing conditions. Further, the similarity in values of both M_∞ and D_x resulting from the different exposures indicates that the interaction between the water molecules and the epoxy network structure is not significantly influenced by the ageing conditions.

Table III provides data related to the activation energy for water diffusion as a result of following the Arrhenius relationship in eq. (3). It is noted that the values of activation energy are fairly close, albeit lower than the value of 16.7 kcal/mol determined through absorption data.

As shown in Table II, the value of M_∞ obtained as a result of desorption using a drying temperature of 40°C is about 4%, which is close to the 3.99% value obtained from the absorption experiments. However, as the drying temperature is increased, M_∞ increases to $\sim$ 4.6% at 60°C and $\sim$ 4.85% at 80°C. The increased value of M_∞ can be related to two phenomena; first, and primarily, a portion of the tightly bound water molecules can be removed only at higher temperatures, and second the higher drying temperatures also have slightly lower levels of humidity in the oven, causing the residual water content after drying to be lower. The higher levels of water removed at the higher drying temperature when compared with the equilibrium moisture content, M_∞, obtained from the absorption tests (as shown in Fig. 2) indicate uptake in the specimens during cure and conditioning.

Dynamic mechanical thermal analysis

DMTA tests were performed to investigate the effects of hygrothermal ageing on the viscoelastic behavior of the polymer. For the purposes of the current investigation, the effects on glass transition temperature (T_g) and the loss tangent (tan δ) curve are emphasized.

Ageing under ambient conditions (23°C and 30% RH)

Figure 5 shows the loss factor (tan δ) curves at various ageing times. It is seen that the peak of the tan δ curve

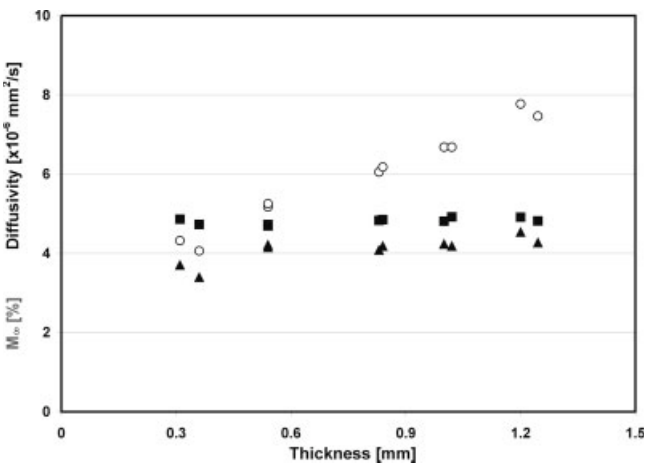

Figure 4 Effect of film thickness on maximum moisture uptake and diffusivity (■, maximum moisture uptake; ▲, D_x; O, D_a).

TABLE II
Moisture Diffusivity and Equilibrium Water Content of the Epoxy Film as a Result of Drying at 40, 60, and 80°C

	Drying at 40°C		Drying at 60°C		Drying at 80°C	
Ageing conditions	M_∞ (%)	D_x (10^{-6} mm^2/s)	M_∞ (%)	D_x (10^{-6} mm^2/s)	M_∞ (%)	D_x (10^{-6} mm^2/s)
23°C, Deionized water	3.93 ± 0.09	0.26 ± 0.01	4.59 ± 0.07	0.87 ± 0.03	4.78 ± 0.05	4.10 ± 0.43
40°C, Deionized water	3.73 ± 0.02	0.27 ± 0.01	4.57 ± 0.05	1.04 ± 0.07	4.76 ± 0.08	4.15 ± 0.21
60°C, Deionized water	4.07 ± 0.04	0.31 ± 0.04	4.81 ± 0.03	0.94 ± 0.04	4.92 ± 0.06	4.12 ± 0.05
23°C, Salt solution	3.97 ± 0.02	0.28 ± 0.04	4.60 ± 0.05	1.05 ± 0.02	4.88 ± 0.07	4.04 ± 0.38
23°C, Alkali solution	4.01 ± 0.16	0.26 ± 0.02	4.60 ± 0.06	0.97 ± 0.03	4.92 ± 0.06	4.38 ± 0.51

moves to higher temperatures and to a lower value, indicating progression of cure over time. As can be seen, T_g initially increases by 7°C over a period of 12 months, at which point moisture uptake is about 0.3%, and then it decreases slightly. The initial increase of T_g indicates that the progression of the postcuring reactions dominates in this period over any plasticization effects that could accrue from moisture uptake. With an increase in time as postcure is largely completed and as the moisture uptake increases, the plasticization effect is likely to be more pronounced causing a slight reduction in T_g. It can be seen in Figure 5 that the height of the tan δ peak gradually decreases with ageing time, reflecting the effects of slow progression of cure under ambient conditions and moisture-induced plasticization. Postcuring enhances the crosslink density and reduces the mobility of the molecular chains indicated by less energy loss in the transition region.[25,26] Moisture present between molecular segments can also reduce segmental interaction also contributing to the decrease.[27]

It was noted that the glassy storage modulus increased slowly with increase in time of ageing, resulting in a change of about 8.6% over the first 6 months and a total of about 32% over the 24-month period of investigation. It is noted that since the change in the glassy modulus is a complex function of the overall resin density, it cannot be directly related to the crosslink density or the moisture content.[28,29] However, the effect of slow progression in cure (also referred to as the postcuring reaction in this article) provides, in any case, a positive effect on the glassy storage modulus.

TABLE III
Activation Energy Under Conditions of Desorption

Ageing conditions	Activation energy (kcal/mol)
23°C, Deionized water	15.06
40°C, Deionized water	14.93
60°C, Deionized water	14.19
23°C, Salt solution	14.61
23°C, Alkali solution	15.46

The activation energy for water uptake is 16.7 kcal/mol.

Ageing in deionized water

Figure 6(a–c) show typical tan δ curves over time resulting from the immersion of specimens in deionized water at 23, 40, and 60°C, respectively, whereas the effects due to immersion in salt and alkali solutions at 23°C are shown in Figure 6(d–e), respectively. As ageing time increases, there is a pronounced shift of the loss tangent peak to lower temperatures, with the maximum shift occurring in the first 6–12 months, representing a decrease in the glass transition temperature which can be related to the effects of plasticization and further modification of the polymer network after extended periods of exposure. As the time of exposure increases, there is an extension of the receding part of the tan δ profile, making it broader and leading to the development of a split in the peak. This response was noted earlier in Refs. 20,28,30–32.

Chateauminois et al.[33] hypothesized that the upper T_g originated from dried region in the samples, which exhibited a T_g close to that of the unexposed material. Akay et al. felt that the time used in DMTA testing was insufficient to cause even partial drying and generation of a new transition and assigned the upper T_g to the inhomogeneous ingress of moisture,[31] wherein regions with very little or no moisture ingress contrib-

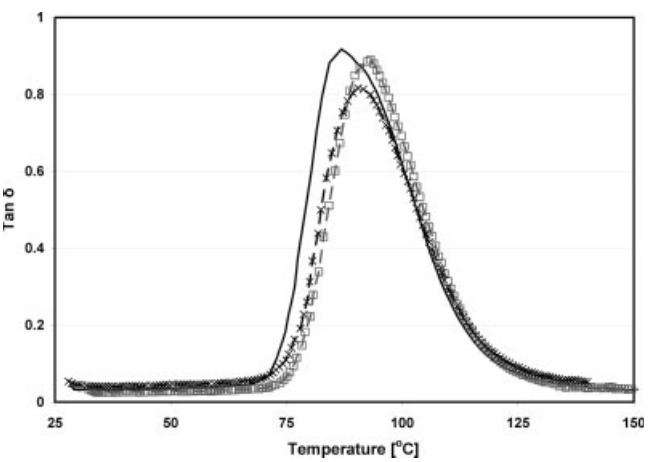

Figure 5 Effect of ageing time under ''control'' conditions (-, 0 months; □, 12 months; -X-, 24 months).

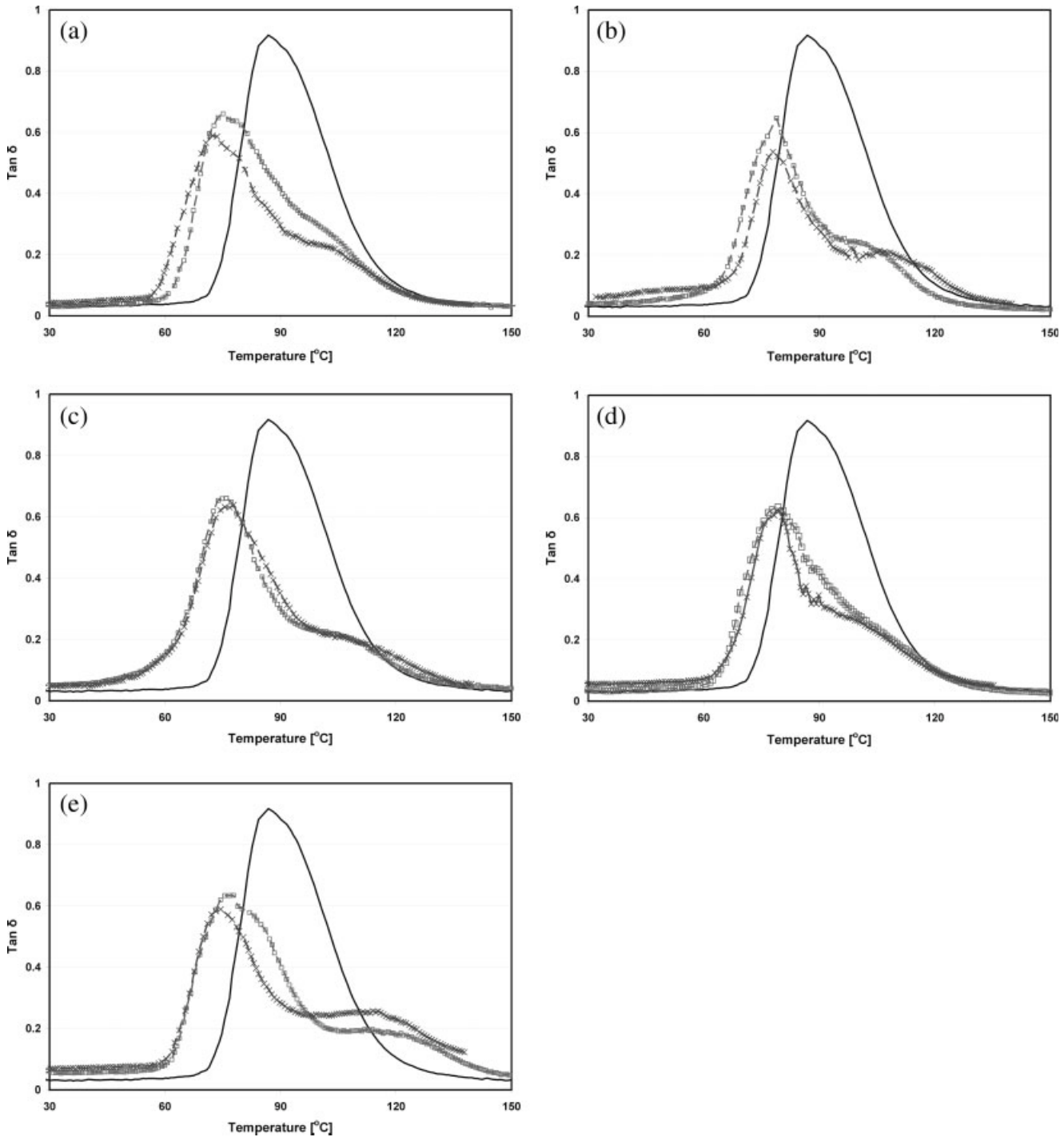

Figure 6 (a) Loss tangent curves as a function of time of immersion in deionized water at 23°C (-, 0 months; □, 12 months; -X-, 24 months). (b) Loss tangent curves as a function of time of immersion in deionized water at 40°C (-, 0 months; □, 12 months; -x-, 24 months). (c) Loss tangent curves as a function of time of immersion in deionized water at 60°C (-, 0 months; □, 12 months; -x-, 24 months). (d) Loss tangent curves as a function of time of immersion in concrete based alkaline solution at 23°C (-, 0 months; □, 12 months; -x-, 24 months). (e) Loss tangent curves as a function of time of immersion in salt water solution at 23°C (-, 0 months; □, 12 months; -x-, 24 months).

ute to the upper T_g. and was previously reported to be due to water which was not chemically linked to the existing polymer network.[20]

If the formation of an upper tan δ peak is related to the drying effect of the temperature ramp during a DMTA test as proposed by Chateauminois et al.,[33] a reduction in thickness of the sample could be expected to lead to a more pronounced upper tan δ peak. However, if the upper peak is due to the inhomogeneous ingress of moisture or from the absorbed

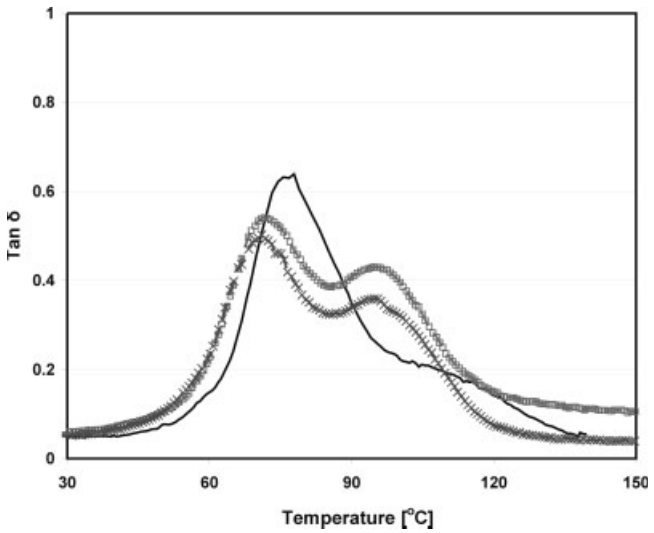

Figure 7 Loss tangent curves related to samples immersed in deionized water at 60°C for 24 months and then tested using a rate of 5°C/min (-, original; □, core; -x-, skin).

water not chemically linked to the polymer network, the amplitude of the upper peak would be independent of the sample thickness. It is noted that as described earlier, moisture uptake in this investigation is independent of the sample thickness.

To address this, two sets of samples (aged at 60°C in deionized water for ~ 2 years) were carefully polished with application of coolant from (a) both sides (denoted as a core sample) or (b) one side (denoted as a skin sample) to a thickness of 2 mm. DMTA experiments were performed on both the skin and core samples, and a comparison of loss tangent curves is presented in Figure 7. It is clear that the upper tan δ peak becomes much more distinct with the decrease in the thickness of samples. The shift of the tan δ peak to the lower temperature for thin samples is directly related to the greater ease of reaching an equilibrium temperature during heating. The skin and core samples show similar tan δ curves, although the heights of the peaks' area slightly different. The weight loss after a run of DMTA test (25–150°C at 5°C/min) is only ~ 0.7% for the initial samples (~ 5 mm in thickness) and ~ 1.2% for the thin samples (~ 2 mm thickness). It was noted that the water molecules at, or very close to, the sample surfaces evaporated rapidly during the DMTA test, and the related epoxy networks exhibit a higher temperature transition leading to the upper tan δ peak.

It was further noted that the use of a slower heating rate (1°C/min as compared to the 5°C/min used earlier) results in a more pronounced upper loss tangent peak. Gravimetric analysis indicated that the samples were almost completely dry after the second DMTA run under the same conditions, with the formation of only a single peak, further supporting the hypothesis that the splitting of the tan δ peak is related to the effect of drying in this case. Examples of this are shown in Figure 8(a–c).

Water uptake by polymers is known to cause plasticization in the short-term and hydrolysis, saponification, and chain scission over the long-term through attack of network linkages. These processes induce higher levels of molecular mobility resulting in consequent decreases in T_g, although the situation can often be complicated by progression of cure due to immersion in aqueous solutions,[34–36] especially at elevated temperatures.[37] As noted in the previous section, the upper T_g is believed to be related to the dried network structures, which in a thicker section would occur close to the surfaces of the sample. For some epoxies, the upper T_g of moist samples and the T_g of dried samples has been shown to be similar.[28,30,33] However, because of the complex interactions between progression of cure and degradation mechanisms occurring during hygrothermal ageing, this cannot be generalized. In the case of the current system, the two T_gs are close in value and thus the upper T_g can be used to approximate the value of the T_g of dried samples.

The change in upper T_g as a function of time of immersion in deionized water at different temperatures is shown in Figure 9. For all the samples immersed in deionized water, the upper T_g increases over the first two periods of exposure (6 and 12 months) after which it levels off. This increase is attributed to slow progression of cure.

The T_g determined from the lower temperature tan δ peak is directly related to the effect of moisture induced plasticization, and the change in these values as a function of time of immersion in deionized water at different temperatures is shown in Figure 10. In direct contrast to Figure 9, the T_g decreases substantially over the first 6 months at all temperatures of immersion with the highest rate of decrease being at the highest temperature of immersion, 60°C. In most cases, the further reduction is extremely slow. The plasticizing effect due to moisture uptake has been widely reported in studies on epoxies and composites. It is noted that there is still considerable uncertainty regarding the exact mechanisms and rates, due to the competing effect of cure progression and moisture induced deterioration.[27,34,35] This issue is further complicated by the fact that dissolution loss of hydrolyzed low molecular weight flexibilizing segments that is known to take place at higher temperatures of immersion over extended periods of time[38] can also cause an increase in T_g after the initial decrease caused by plasticization and hydrolysis. It is noted that samples immersed in deionized water at 60°C show the initial decrease, followed by an increase, indicating this type of response.

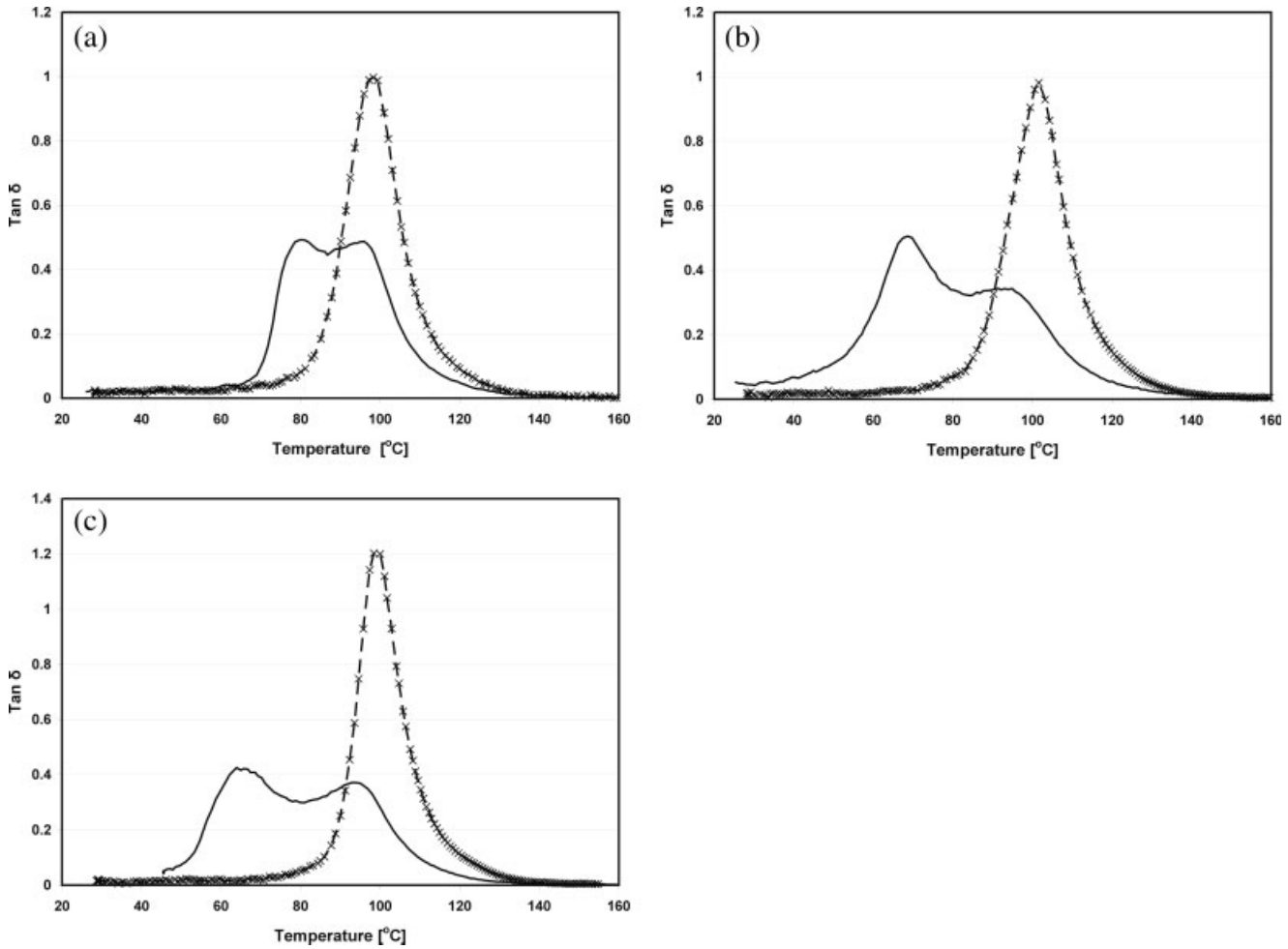

Figure 8 (a) Effect of multiple DMTA runs on loss tangent curve for specimens immersed in water at 23°C (-, first run; -x-, second run). (b) Effect of multiple DMTA runs on loss tangent curve for specimens immersed in water at 60°C (-, first run; -x-, second run). (c) Effect of multiple DMTA runs on loss tangent curve for specimens immersed in concrete based alkali solution at 23°C (-, first run; -x-, second run).

Because of the competing effects of cure progression and moisture induced deterioration, including leaching, it is difficult to directly evaluate the relation, if any, between moisture content and deteriorative mechanisms in the initial stages of ageing. To assess this aspect further, specimens aged in deionized water for two years were dried to varying moisture contents. These were then characterized using DSC and the results are shown in Figure 11. As can be seen, the T_g decreases almost linearly with moisture content, irrespective of temperature of immersion with the decrease being in line with the free volume theory which in simplified form can be expressed as[9]

$$\frac{1}{T_g} = \frac{1}{T_{\mathrm{gp}}} + \left(\frac{1}{T_{\mathrm{gw}}} - \frac{1}{T_{\mathrm{gp}}}\right)v \tag{5}$$

where T_g is the wet glass transition temperature, T_{gp} is the dry glass transition temperature, T_{gw} is the glass transition temperature of water, and ν is the

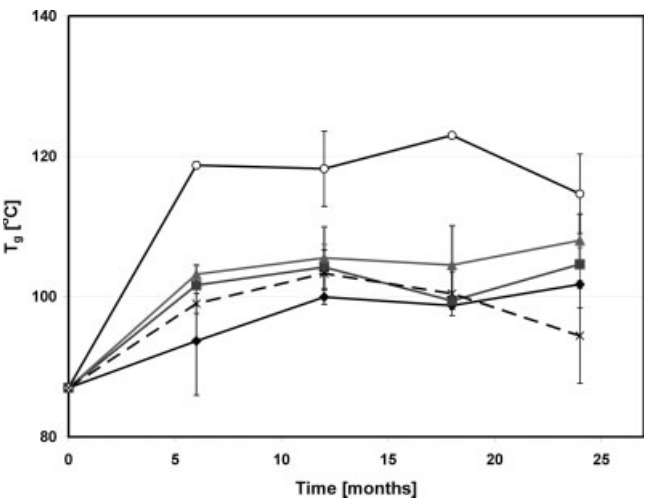

Figure 9 Effect of type of environment and period of immersion on upper T_g (◆, deionized water at 23°C; ■, deionized water at 40°C; ▲, deionized water at 60°C; X, alkali solution at 23°C; O, salt solution at 23°C).

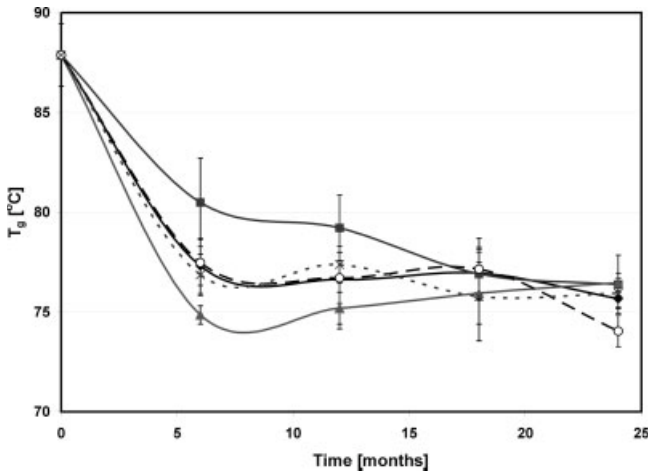

Figure 10 Lower T_g as a function of ageing time (◆, deionized water at 23°C; ■, deionized water at 40°C, ▲, deionized water at 60°C; X, alkali solution at 23°C; O, salt solution at 23°C).

water content expressed in terms of volume fraction $\left(v = w\frac{\rho}{\rho_w}\right)$ where w is the weight fraction of water determined from uptake, ρ is the density of the moist epoxy and ρ_w is the density of water. Using eq. (5) in conjunction with the data in Figure 11, the glass transition temperature of water is obtained as 142.85 K which is well within the reported range of 100–150 K[21] and close to the simulated value of 165 K recently reported by Giovambattista et al.,[39] confirming that the plasticizing effect in the current case can be described by the free volume theory.

DSC tests were also conducted on already dried samples in two runs in sequence with heating from 25 to 160°C at 10°C/min, and cooling between the runs at a rate of 2°C/min. As shown in Figure 12, the T_g related to the second run is lower than that obtained in the first run which matches the trends reported from the DMTA characterization in Table IV. From the values of the storage modulus in the rubbery phase, it can be clarified that the heating and cooling regimes did not cause an obvious degradation in the dried epoxy samples. It is, however, known that water molecules tightly bound to the network can act as intermolecular joints exhibiting an antiplasticization response.[18] The temperature regime applied through the DSC after drying is hypothesized to cause removal of these molecules resulting in the subsequent drop in T_g. This hypothesis for the removal of the tightly bound water molecules is supported by the weight loss of 0.3–0.5% that was ascertained to have taken place as a result of the DSC treatment. Further research on this through carefully controlled experiments initiated soon after processing and as a function of time of immersion are ongoing and will be reported at a later date.

Ageing in salt and alkaline solutions

Figures 9 and 10 show the effects of ageing in salt and concrete based alkaline solutions on the upper and lower T_gs, respectively. As can be seen in Figure 9, the immersion in salt water results in a rather substantial change in the value of the upper T_g beyond that seen through immersion in deionized water at the same temperature (23°C) which follows earlier results reported by Wu et al.[40] To further investigate the reason for this anomalous behavior, sets of specimens immersed in salt water for 24 months were cut into 0.5-mm thick films and DMTA tests were conducted on core and skin specimens after drying them at 60°C for 48 h. Representative results from this set of tests are shown in Figure 13(a) wherein the core

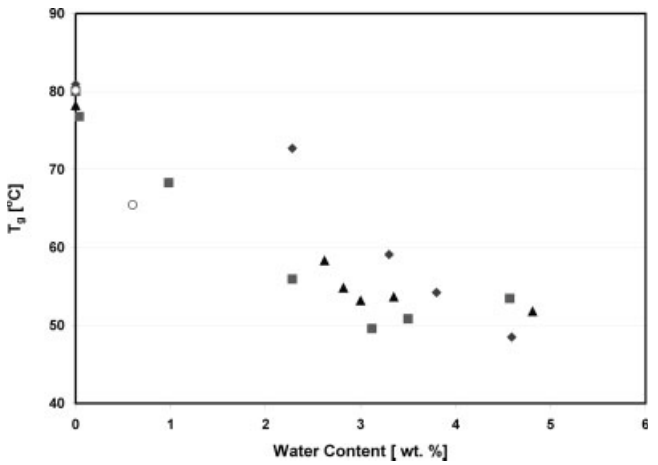

Figure 11 T_g (determined through DSC analysis) as a function of moisture content (◆, deionized water at 23°C; ■, deionized water at 40°C; ▲, deionized water at 60°C; ○, control).

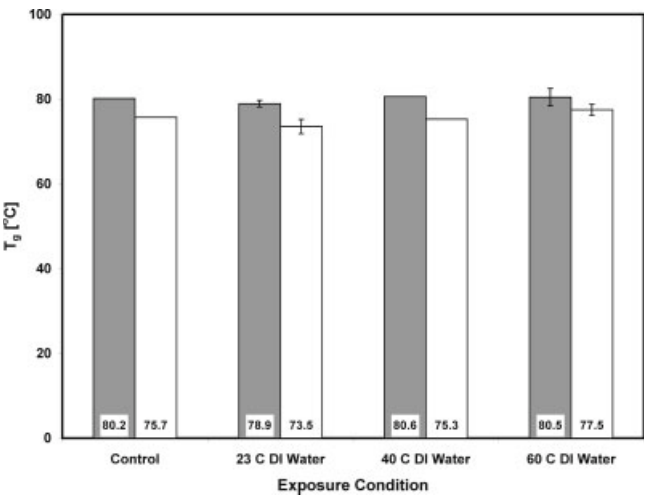

Figure 12 T_g of samples as measured by DSC after drying (shaded, run 1; blank, run 2).

TABLE IV
Change in T_g (Measured from the Peak of the Tan δ Curve) of 60°C-Dried Epoxy Samples Measured Before and After High Temperature Treatment[a]

Immersion conditions	T_g before treatment (°C)	T_g after treatment (°C)	Weight loss (%)
23°C, Deionized water	101.3	100.3	0.52
40°C, Deionized water	100.5	97.4	0.51
60°C, Deionized water	102.3	99.2	0.5
23°C, Alkali solution	99.1	97	0.44
23°C, Salt solution	98.7	95.7	0.31

[a] Consequent ramps of 5°C/min from 25 to 160°C with intermediate cooling at about 2°C/min.

samples show response that is typically seen from specimens aged under all other conditions (deionized water and alkaline solution), while the skin samples show two distinct transitions with a lowered transition saddle. The transitions, while not as apparent, can also be seen in the traces for storage modulus [Fig. 13(b)]. Since the films were completely dried prior to testing, these transitions appear to indicate the formation of two distinct network structures formed in the skin region with one having a higher level of crosslinking (which contribute to the upper tan δ peaks) than that seen in the bulk (as indicated by the core samples) and the other having a lower level of crosslinking. Preliminary studies indicate that this biphasic structure indicates differently plasticized phases which could be due to the effects of migration of ions from the salt solution with the overall effect of deterioration not being completed in the 24-month period of immersion. The core is not affected within this period, since the ions have not migrated beyond the skin regions within the period of immersion studied. Further studies are ongoing to elucidate these mechanisms. It is noted that the changes in lower T_g follow those due to immersion in deionized water at the same temperature (23°C) very closely, with the only difference being in the last period of immersion (between 18 and 24 months) where there is a clear decrease in T_g related to specimens immersed in the salt water solution, indicating further irreversible deterioration.

In comparison, immersion in the concrete based alkali solution is seen to cause a significant decrease in the value of the upper T_g after the 12 month period of immersion, and a smaller decrease in the value of the lower T_g. Both these, in conjunction with the lowering of the tan δ peak and shifting to the left after exposure, suggest increased plasticization and hydrolysis in the polymer.

SUMMARY

In light of the increasing reliance on externally bonded FRP composites for the strengthening of deteriorating and under-strength concrete structural components, there is a critical need to characterize and understand the hygrothermal ageing response of am-

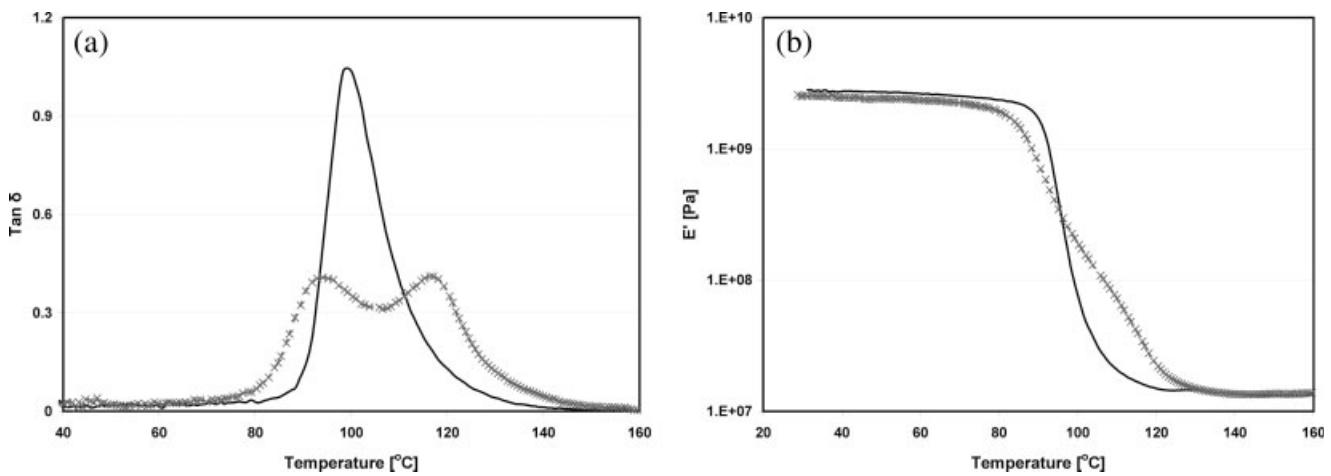

Figure 13 (a) Differentiation between loss tangent profiles from DMTA characterization after drying of skin and core sections of specimen immersed in salt solution for 24 months (-, core; -x-, skin) (b) Differentiation between storage modulus profiles from DMTA characterization after drying of skin and core sections of specimen immersed in salt solution for 24 months(-, core; -x-, skin).

bient temperature cure resin systems used in such processes. The system investigated exhibits primarily Fickian response with the diffusion coefficient increasing with the temperature of immersion in deionized water. The effect of immersion in 5% NaCl solution and concrete based alkali solution is almost identical to that obtained from immersion in deionized water at the same temperature of 23°C. Maximum (i.e., equilibrium) moisture content in all solutions is seen to converge to the same level, and the activation energy in deionized water is found to be 16.7 kcal/mol.

Through DMTA characterization postcuring is noted to continue for a period of time with the effect dominating over that of plasticization in the early stages of immersion. Splitting of the loss tangent curves for specimens immersed in deionized water and alkali solution indicates the formation of biphasic structures and drying of the network structure. Postimmersion high temperature exposure (drying) reveals the removal of tightly bound water molecules, resulting in a decrease of the glass transition temperature. The use of DSC tests on postimmersion samples dried to various levels enables the determination of a relationship between glass transition temperature and moisture content from which the glass transition temperature of water is obtained as 142.85 K, confirming that the plasticizing effect in the current case can be described by the free volume theory.

References

1. Adamson, M. J. J Mater Sci 1980, 15, 1736.
2. Neumann, S.; Marom, G. Polym Compos 1985, 6, 9.
3. Colombini, D.; Martinez-Vega, J. J.; Merle, G. Polymer 2002, 43, 4479.
4. Apicella, A.; Nicolais, L. Adv Polym Sci 1985, 72, 69.
5. Tcharkhtchi, A.; Bronnec, P. Y.; Verdu, J. Polymer 2000, 41, 5777.
6. Bellenger, V.; Verdu, J.; Morel, E. J Mater Sci 1989, 24, 63.
7. Morel, E.; Bellenger, V.; Verdu, J. Polymer 1985, 26, 1719.
8. Merdas, I.; Tcharkhtchi, A.; Thominette, F.; Verdu, J.; Dean, K.; Cook, W. Polymer 2002, 43, 4619.
9. Merdas, I.; Thominette, F.; Tcharkhtchi, A.; Verdu, J. Compos Sci Technol 2002, 62, 487.
10. Crank, J. The Mathematics of Diffusion, 2nd ed.; Clarendon: Oxford, UK, 1975.
11. Crank, J.; Park, J. S. Diffusion in Polymers; Academic Press: New York, 1968.
12. Frisch, H. L. J Chem Phys 1964, 41, 3379.
13. Carter, H. G.; Kibler, K. G. J Compos Mater 1978, 12, 118.
14. Zhou, J. M.; Lucas, J. P. Polymer 1999, 40, 5505.
15. Boinard, P.; Banks, W. M.; Pethrick, R. A. Polymer 2005, 46, 2218.
16. Antoon, M. K.; Koenig, J. L.; Serafini, T. J Polym Sci Polym Phys Ed 1981, 19, 1567.
17. Woo, M.; Piggott, M. R. J Compos Technol Res 1987, 9, 101.
18. Zhou, J. M.; Lucas, J. P. Polymer 1999, 40, 5513.
19. Karbhari, V. M.; Murphy, K.; Zhang, S. J Compos Mater 2002, 36, 2101.
20. Deneve, B.; Shanahan, M. E. R. Polymer 1993, 34, 5099.
21. Pascault, J.-P.; Sautereau, H.; Verdu, J.; Williams, R. J. J. Thermosetting Polymers; Marcel Dekker: New York, 2002.
22. Bao, L. R.; Yee, A. F. Compos Sci Technol 2002, 62, 2099.
23. Chin, J. W.; Nguyen, T.; Aouadi, K. J Appl Polym Sci 1999, 71, 483.
24. Abanilla, M. A.; Li, Y.; Karbhari, V. M. Compos B 2006, 37, 200.
25. Ishisaka, A.; Kawagoe, M. J Appl Polym Sci 2004, 93, 560.
26. Chang, T. D.; Carr, S. H.; Brittain, J. O. Polym Eng Sci 1982, 22, 1213.
27. Karbhari, V. M. J Reinforc Plast Compos 2006, 25, 631.
28. Ivanova, K. I.; Pethrick, R. A.; Affrossman, S. J Appl Polym Sci 2001, 82, 3477.
29. Hough, J. A.; Xiang, Z. D.; Jones, F. R. In Experimental Techniques and Design in Composite Materials 3; Priolo, P., Ed.; Trans Tech Publications: Switzerland, 1998; p 27.
30. Akay, M.; Mun, S. K. A.; Stanley, A. Compos Sci Technol 1997, 57, 565.
31. Soulier, J. P.; Berruet, R.; Chateauminois, A.; Chabert, B.; Gauthier, R. Polym Commun 1988, 29, 243.
32. Karad, S. K.; Attwood, D.; Jones, F. R. Compos Appl Sci Manuf 2002, 33, 1665.
33. Chateauminois, A.; Chabert, B.; Soulier, J. P.; Vincent, L. Polym Compos 1995, 16, 288.
34. Ghorbel, I.; Valentin, D. Polym Compos 1993, 14, 324.
35. Marshall, J. M.; Marshall, G. P.; Pinzelli, R. F. Polym Compos 1982, 13, 131.
36. Karbhari, V. M.; Zhang, S. Appl Compos Mater 2002, 10, 19.
37. Schultheisz, C. R.; Schutte, C. L.; McDonough, W. G.; Macturk, K. S.; McAuliffe, M.; Kodagunta, S.; Hunston, D. L. In ASTM STP 1290; Spragg, C. J.; Drzal, L. T., Eds.; ASTM: Conschoken, PA, 1996; p 103.
38. Apicella, A.; Migliaresi, C.; Nicolais, L.; Iaccarino, L.; Roccotelli, S. Composites 1983, 14, 387.
39. Giovambattista, N.; Angell, C. A.; Sciortino, F.; Stanley, H. E. Phys Rev Lett 2004, 93, 047801.
40. Wu, L.; Murphy, K.; Karbhari, V. M.; Zhang, J. S. J Appl Polym Sci 2002, 84, 2760.